Impacts of Morphological Characteristics on Target Strength of Chub Mackerel (*Scomber japonicus*) in the Northwest Pacific Ocean

Jianfeng Tong[1,2,3,4]*, Minghua Xue[1], Zhenhong Zhu[1], Weiqi Wang[1] and Siquan Tian[1,2,3,4]

[1] College of Marine Sciences, Shanghai Ocean University, Shanghai, China, [2] National Engineering Research Center for Oceanic Fisheries, Shanghai Ocean University, Shanghai, China, [3] Key Laboratory of Sustainable Exploitation of Oceanic Fisheries Resources, Ministry of Education, Shanghai, China, [4] Key Laboratory of Oceanic Fisheries Exploration, Ministry of Agriculture and Rural Affairs, Shanghai, China

Chub mackerel (*Scomber japonicus*) is an important commercial fish in the Northwest Pacific Ocean. Accurate target strength (*TS*) underpins acoustic stock assessment but the *TS* of *S. japonicus* is still poorly understood. In this study, the Kirchhoff-ray mode (KRM) model was used to estimate the *TS* of *S. japonicus* and its relationship with sound wave frequency and fish morphology. The results revealed that *TS* values varied with pitch angle shifts, with the impact on fish scattering strength being greater at higher frequency. This is less important because 38 kHz has been used for the biomass assessment of these fish resources. At frequencies of 38 kHz, 70 kHz, 120 kHz and 200 kHz, *TS* was greatest at a pitch angle range of -10° to 0°, which was related to the angle of the swim bladder tilt. There were almost no differences between *TS* estimated using the measured pitch angle distributions and using the universal distribution. When the measured pitch angle was *N* [-3°,4°], the average *TS* of *S. japonicus* with body length of 12.04–22.17 cm at four frequencies was -48.88 dB, -49.14 dB, -49.75 dB and -48.55 dB, respectively. The regression intercept (b_{20}) in *TS*–body length equation was -73.27 dB, -73.56 dB, -74.18 dB and -73.46 dB, respectively. Variation in *TS* range at 0–300 m depth was about 10 dB. The simulated broadband target strength spectrum shows the scattering characteristics of individuals with different swim bladder length between 0–250 kHz. These results could be used for identification of *S. japonicus* in echograms and provide reference for acoustic stock assessment of *S. japonicus* in the Northwest Pacific Ocean.

Keywords: Kirchhoff-ray mode model, target strength, *Scomber japonicus*, Northwest Pacific Ocean, acoustic

INTRODUCTION

The Northwest Pacific Ocean has abundant fishery resources (Chiba et al., 2009; Miyamoto et al., 2020). As the most productive marine fishery area in the world, total catches in this area reached 20.06 million tons in 2018, accounting for 23.76% of total marine catches (FAO, 2020). Chub mackerel (*Scomber japonicus*) is a warm-water pelagic fish. As one of the most economically

important fish species in the Northwest Pacific Ocean, it plays an important role in the marine fisheries of China, Japan, and South Korea. Total global catch of *S. japonicus* was 1.56 million tons in 2018, accounting for 2% of total marine catches (FAO, 2020). However, *S. japonicus* biomass has declined sharply since 1997 and has remained low over the past few decades (Takahashi et al., 2014). To develop appropriate fishery management measures and sustainably use *S. japonicus* resources, it is necessary to assess its biomass accurately.

Underwater acoustic surveys can provide high-resolution information in large-scale bodies of water and are widely used in monitoring behavior of marine organisms (Muñoz et al., 2020), habitat distribution research (Zhang et al., 2020), and stock assessment (Stierhoff et al., 2019; Escobar-Flores et al., 2020). Target strength (*TS*) is a key parameter used to identify species in the echogram and convert the echo signal into biomass. *TS* varies between species and is affected by many factors including swim bladder characteristics (Foote, 1980), body size (Lu et al., 2011), swimming pitch angle (Horne, 2003), water depth (Mukai and Iida, 1996), and incident sound wave frequency (Foote, 1982). Therefore, it is very important to correctly identify target species, estimate their *TS*, and understand the factors that affect *TS* variation to accurately assess stocks of marine fish.

Estimation methods of *TS* mainly include *in situ*, *ex situ*, and theoretical models (Sobradillo et al., 2021). The *in situ* method records the *TS* of fish in their natural environment. This method requires the target fish to be discretely distributed and single-species (Simmonds and MacLennan, 2005). However, these conditions are difficult to satisfy, especially in mixed species aggregations. The *ex situ* method measures the *TS* of target fish in an artificial acoustic experimental arena; however, the experimental arena is challenging to set up and has poor flexibility. Theoretical models approximate the main source of acoustic scattering to a regular geometric model based on scattering theories and biological characteristics of the fish. Then, computer simulations are used to estimate *TS*. Because the model method is simple, flexible and low-cost, it could enable the study of the factors affecting *TS* (Hazen and Horne, 2003). Additionally, theoretical models could improve the ability to identify and classify targets in echograms (Jech and Horne, 2002) and reduce the uncertainty of stock assessment (Khodabandeloo et al., 2021).

The Kirchhoff-ray mode (KRM) model could simulate the process of sound waves from seawater into the body and swim bladder of fish. It uses low-mode solutions and Kirchhoff-ray approximations to estimate resonant and geometric backscatter from the body and swim bladder of fish (Gauthier and Horne, 2004). The results of the KRM model are consistent with those of *in situ* and *ex situ* methods (Horne, 2003; Kang et al., 2004; Kusdinar et al., 2014). Some researchers have used the KRM model to study the effects of different factors on *TS*. For example, Hazen and Horne (2003) used KRM to determine that pitch angle and frequency had greater effects on walleye pollock (*Theragra chalcogramma*) *TS* compared to length, while depth had the least effect. Gauthier and Horne (2004) established the

TS–length equation for five pelagic fish species in the Bering Sea and the Gulf of Alaska.

The purpose of this study was to estimate the impacts of morphological characteristics on the *TS* of *S. japonicus* in the Northwest Pacific Ocean, so as to improve the acoustic stock assessment accuracy. First, the morphological characteristics of the swim bladder and its changes with fish growth were described based on X-ray images. Then, the KRM model was used to calculate the *TS* of *S. japonicus* and to analyze variation in *TS* with fish body and swim bladder shape at different frequencies. Four common frequencies used in acoustic fishery surveys, including 38 kHz, 70 kHz, 120 kHz and 200 kHz, were selected. Finally, a broadband *TS* spectrum was produced by simulating the variation of *TS* with frequency in the range of 0–250 kHz. Our work could provide a scientific basis for signal identification of *S. japonicus* in echograms and provide reference for acoustic stock assessment of *S. japonicus* in the Northwest Pacific Ocean.

MATERIALS AND METHODS

Field Sampling
Samples were obtained from 147°E–165°E, 33°N–44°N in the Northwest Pacific Ocean by the Shanghai Ocean University research vessel (RV) Songhang. The survey was conducted from June 18 to August 7, 2021 using a four-panel midwater trawl with a mean speed of 4.6 knots. Samples were frozen in seawater immediately after being captured and stored in plastic bottles at -20°C onboard the research vessel.

Morphological Measurements
One month after capture, frozen samples were transferred to the laboratory. There, the bottles were slowly thawed in cold water over a period of 20 h to minimize any changes in swim bladder shape (Yasuma et al., 2010). After the length and weight measurements of samples were recorded, a specialized MIKASA HF100HA X-ray imaging system, with input voltage of AC220 V maximum tube voltage of 100 kV, and maximum tube current of 40 mA, was used to map the outlines of each fish. Both lateral and dorsal aspects from 18 individuals were X-rayed. Morphological parameters of each sample were measured as shown in **Figure 1**, including body length (*BL*), body height (*BH*), body width (*BW*), swim bladder length (*SL*), swim bladder height (*SH*) and swim bladder width (*SW*). The swim bladder tilt angle was also measured relative to the main axis of the lateral image aspect.

TS Estimation
Since the lack of *in situ* data, the KRM model (Clay and Horne, 1994) was used to estimate *TS*. Acoustic parameters, such as the density contrast (*g*) and sound speed contrast (*h*), were needed in this model. Previous researchers found that fish flesh had *g* values ranging from ~1.02 to 1.06 and *h* values from ~1.02 to 1.08 (Love, 1978; Medwin and Clay, 1998; Gastauer et al., 2016). Typical acoustic parameters of fish with a swim bladder, measured using Atlantic cod (*Gadus morhua*), from literature
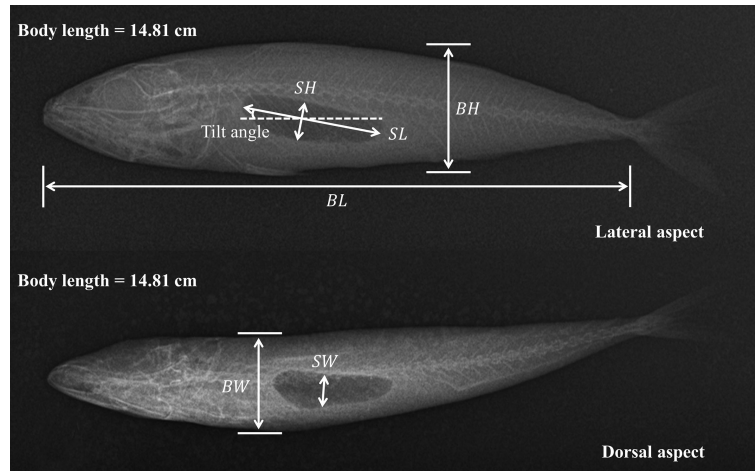
FIGURE 1 | Morphological measurements on lateral and dorsal X-ray images. The air-filled swim bladder can be seen as a dark shape within the fish body. The symbols *BL, BH* and *BW* represent body length, body height, and body width, respectively. While the symbols *SL, SH* and *SW* represent swim bladder length, swim bladder height, and swim bladder width, respectively.

(Clay and Horne, 1994) were chosen in our model (**Table 1**), which were also used in the jack mackerel (*Trachurus japonicus*) *TS* research performed by Hwang et al. (2015). *TS* of fish is closely related to the sound wave frequency and the swimming pitch angle. Broadband scattering characteristics with a frequency in the range of 0–250 kHz were simulated to plot the entire broadband *TS* spectrum. According to Yasuma et al. (2003), when the incidence sound wave is perpendicular to the dorsal aspect of the fish body, the pitch angle is defined as 0°. Shifts in *TS*, when the swimming pitch angle ranged from −50° (head-down) to 50° (head-up), were estimated at frequencies of 38 kHz, 70 kHz, 120 kHz, and 200 kHz. Average *TS* value was calculated from estimated *TS* across the pitch angle distribution. This value was used as the *TS* of individual fish (Yasuma et al., 2010). Pitch angle follows a normal distribution defined by $N[\bar{\theta}, Std]$ where $\bar{\theta}$ is the mean pitch angle and *Std* is the standard deviation (Furusawa, 1988; Bairstow et al., 2021). In this paper, three previously determined pitch angle distributions were used. Two of them were observed from *S. japonicus*, $N[−3°,4°]$ (Nauen and Lauder, 2002) and $N[−0.5°,0.09°]$ (Gibb et al., 1999), while another one was a universal distribution calculated from many species, $N[−5°,10°]$ (Kusdinar et al., 2014; Sun et al., 2021). The average *TS* of *S. japonicus* could be calculated as follows:

$$\overline{TS} = 10 \log_{10} \bar{\sigma} \tag{1}$$

Where $\overline{TS}$ is the average *TS* of all *S. japonicus* samples, and $\bar{\sigma}$ is the average backscattering cross-section of all samples. According to Boyle's law (Scoulding et al., 2015; Proud et al., 2019), the following model (Sobradillo et al., 2019) was used to estimate *TS* variation relative to depth:

$$\sigma_z = \bar{\sigma}\left(1 + \frac{z}{10}\right)^{\alpha} \tag{2}$$

where σ_z is the backscattering cross-section at depth *z*, and *a* is the estimated contraction rate whose value is −0.67 for a free ellipsoid (Ona, 2003).

The relationship between *TS* and body length at four frequencies was analyzed using the least-squares method. *TS*–body length equation could be expressed as:

$$TS = a \log_{10} BL + b \tag{3}$$

where *a* is the slope of the regression, *b* is the intercept, and *BL* represents body length. According to Furusawa (1988), equation (3) could be transformed into:

$$TS = 20 \log_{10} BL + b_{20} \tag{4}$$

where b_{20} is the intercept when a=20.

TABLE 1 | Acoustic parameters used in the KRM model of the *TS* of *S. japonicus*.

Description	Value	Unit
Density of sea water	1030	kg/cm³
Density of fish body	1070	kg/cm³
Density of swim bladder gas	1.24	kg/cm³
Sound speed of sea water	1490	m/s
Sound speed in fish body	1570	m/s
Sound speed in swim bladder	345	m/s

Parameters were taken from Clay and Horne (1994) for cod.

RESULTS

Morphology of *S. japonicus*

The range of body length of the 18 *S. japonicus* was 12.98–22.17 cm, with a mean of 16.08±3.15 cm (mean ± SD). The range of swim bladder length was 1.45–6.63 cm, with a mean of 3.64 ± 1.49 cm. Tilt angle was from 1.7° to 14.0° and mean tilt angle was 8.26° ± 3.62°.

TS Variation With Body Pitch Angle Shifts

Figure 2 shows *TS* variation of each sample in relation to pitch angle shifts. We used ΔTS (TS_{max}-TS_{min}) to represent this variation. When pitch angle shifted from −50° to 50°, the ΔTS range of the 18 *S. japonicus* at four frequencies was 12.33–52.68 dB, 28.81–45.34 dB, 26.38–52.30 dB, and 28.57–50.15 dB, respectively.

At the same frequency, body length did not affect ΔTS of *S. japonicus*. **Figure 3** details *TS* variation related to body, swim bladder, and the whole fish (*BL*=14.81*cm*) relative to pitch angle shifts. Observed variation in *TS* relative to whole fish was consistent with the observed variation of swim bladder *TS*, but not that of the body. *TS* was significantly affected by the pitch angle and varied greatly with frequency. At a frequency of 38 kHz, 70 kHz, 120 kHz, and 200 kHz, *TS* peaked (main lobe) around −10° to 0°. As frequency increased, the main lobes

increased directionality, the number of side lobe peaks and fluctuation increased. These results suggest that the impact of fish behavior on scattering strength becomes greater with increasing frequency.

Average *TS*

Average *TS* of each sample with different pitch angle distributions was estimated using the KRM model. The difference in average *TS* between the samples with the largest and smallest body length was about 10 dB. Small differences, nearly 1 dB, were observed among the average *TS* of individuals between each frequency. *TS* was estimated using the measured *S. japonicus* angle distributions *N*[−3°,4°] and *N*[−0.5°,0.09°], and the universal distribution *N*[−5°,10°] was almost identical. Differences between three distributions had little effect on the KRM results in this study.
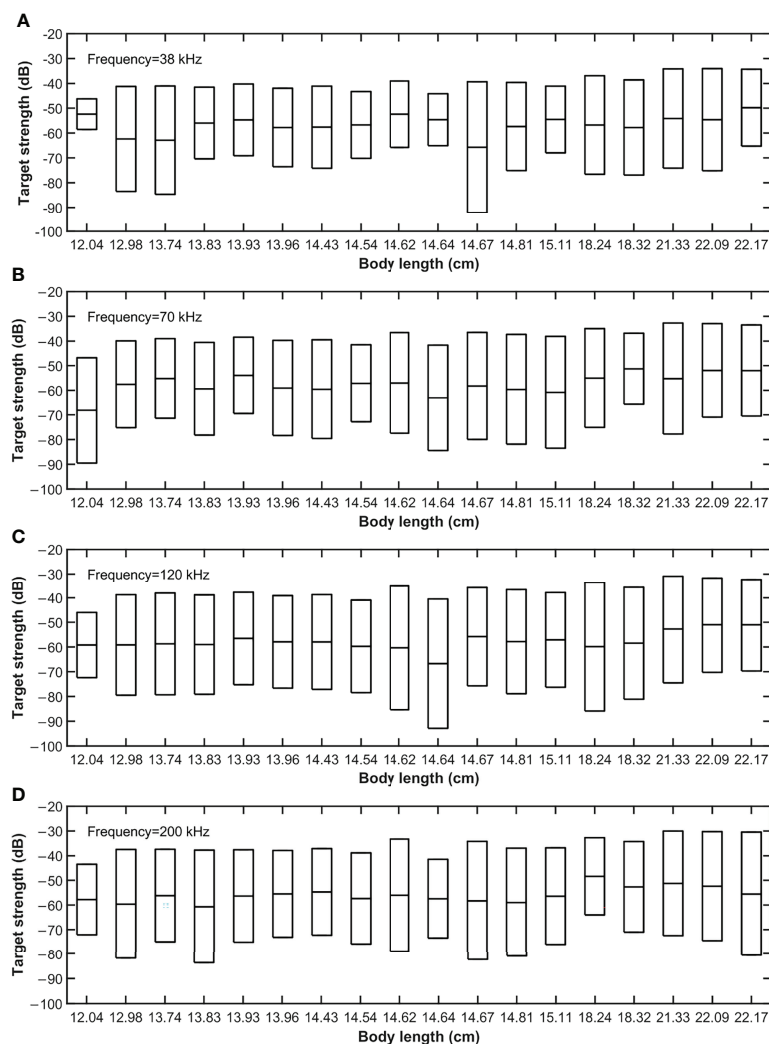

FIGURE 2 | Variation in *TS* of each sample with pitch angle ranging from -50° to 50°. Using ΔTS, the difference between the maximum TS and the minimum TS, to represent the variation values. The range of ΔTS was: **(A)** 12.33–52.68 dB at 38 kHz; **(B)** 28.81–45.34 dB at 70 kHz; **(C)** 26.38–52.30 dB at 120 kHz; **(D)** 28.57–50.15 dB at 200 kHz. Top and bottom edges of the box represent maximum and minimum values of TS, respectively. The middle line is the half of ΔTS.
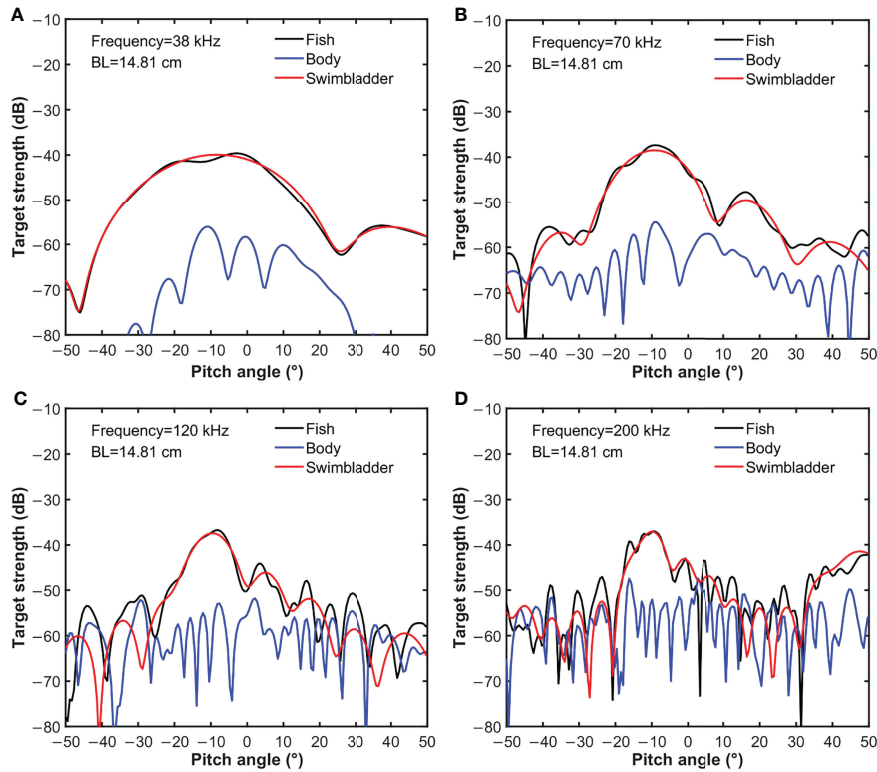
FIGURE 3 | *TS* variation of body, swim bladder, and the whole fish (BL=14.81*cm*) with pitch angle shifts at **(A)** 38 kHz, **(B)** 70 kHz, **(C)** 120 kHz and **(D)** 200 kHz.

Table 2 shows the $\overline{TS}$ values of all *S. japonicus* at 38 kHz, 70 kHz, 120 kHz, and 200 kHz frequencies with different pitch angle distributions. The difference of the $\overline{TS}$ between each frequency was about 1 dB, no matter which distribution was used.

S. japonicus usually lives in 0–300 m depth. **Figure 4** shows *TS* variation relative to depth when angle distribution is *N* [−3°,4°]. *TS* decreased gradually as water depth increased. When the size of the swim bladder decreases due to pressure, the *TS* of the fish also decreases This phenomenon was greatest in depths of 0–60 m. The decrease slowed down in water deeper than 60 m and stabilized at 300 m. The shift range of *TS* from 0–300 m depth was about 10 dB.

TS-BL Equation

The relationship between *TS* for average pitch angle and body length of *S. japonicus* is shown in **Figure 5**. The equations for the linear regression in **Figure 5** are listed in **Table 3**.

TS increased along with body length at different frequencies. However, the fitted *TS-BL* equations always differed from the standard equations. As shown in **Table 3**, the regression slopes (a) were greater than 20 in all cases. This suggests that the backscattering cross-section of *S. japonicus* is not proportional to the square of body length and that the *TS* increases at a greater rate than body length. There were almost no differences between the b_{20} values estimated using the measured pitch angle distributions and the values estimated by using the universal distribution. The intercept and slope of the *TS-BL* equation was

affected by frequency. For example, *TS* increased the least with *BL* at 38 kHz and the most at 200 kHz. The b_{20} decreased with frequency increasing.

The Broadband Scattering Characteristics

The broadband *TS* spectrum of the 18 *S. japonicus*, estimated using the pitch angle distribution *N*[−3°,4°], in the frequency range of 0–250 kHz, is shown in **Figure 6**. *TS* values decreased along with swim bladder length but the resonance frequency dominated by Rayleigh scattering increased. As frequency increased and entered into the Mie scattering range, *TS* began to fluctuate over a range of 5 dB. However, individuals with

TABLE 2 | $\overline{TS}$ values for different pitch angle distributions at four frequencies.

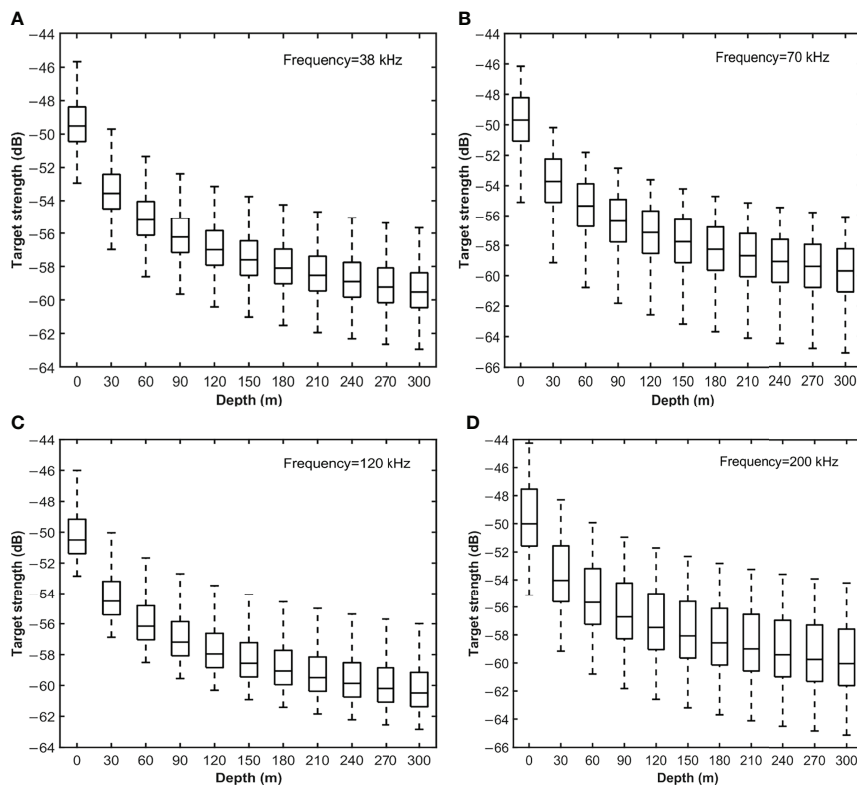| Pitch angle distribution	Frequency (kHz)	$\overline{TS}$ (dB)
N[-5°,10°]	38	-49.14
	70	-49.41
	120	-50.01
	200	-48.81
N[-3°,4°]	38	-48.88
	70	-49.14
	120	-49.75
	200	-48.55
N[-0.5°,0.09°]	38	-48.70
	70	-48.96
	120	-49.56
	200	-48.37

FIGURE 4 | *TS* variation relative to depth when the angle distribution is *N*[−3°,4°] at **(A)** 38 kHz, **(B)** 70 kHz, **(C)** 120 kHz and **(D)** 200 kHz. On each box, the central line indicates the median *TS* value of all samples. The bottom and top edges of the box indicate the 25th and 75th percentiles, respectively. The whiskers extend to the most extreme data without outliers.

different swim bladder lengths showed two trends after 150 kHz. *TS* of fish whose *SL>3 cm* increased, while the *TS* of fish with *SL>3 cm* maintained stability.

DISCUSSION

The KRM model requires precise measurements of the body and swim bladder to obtain detailed morphological parameters. Therefore, we used a specialized X-ray imaging system to map the outlines of the fish, which reliably reflects the size of the swim bladder and its relative position in the body. Sample preservation quality greatly influenced image quality as the swim bladder may not be obvious in the poorly preserved samples. In this study, *S. japonicus* samples were collected *in situ* and frozen in seawater, ensuring the relative stability of the internal structure of the fish and improved measurement accuracy. However, morphology will inevitably change during freezing and thawing, and temperature cannot be kept constant during long periods of time needed for transportation. Sobradillo et al. (2019) proposed using liquid nitrogen to freeze samples and thaw them in a temperature-controlled environment (0°C), which can minimize damage to biological structures. It is better to take X-rays *in situ* when conditions permit, to avoid freezing and transportation.

The total catch of *S. japonicus* during the survey period was 1,299 and their body length distribution follows *N*[16.15,4.14]. Among these catches, 946 individuals with gonadal maturity of stage 1 and stage 2 indicate that they were mainly juveniles. In this paper, the body length distribution of the 18 samples was *N*[15.86,3.15], which is consistent with the overall catches. Although there were few samples used in *TS* estimation, it would not have a large impact on conclusions.

The *TS* of fish is influenced by many factors. There are even differences in the same species due to variation in individual morphology. The size of this difference depends on the frequency of the sound waves (Gauthier and Horne, 2004). At 38 kHz, *TS* was relatively stable with body pitch angle shifts and there were fewer side lobes. While at higher frequencies, wavelength interaction in the body produced more interference which caused greater fluctuation in *TS* and more side lobes. *TS* of *S. japonicus* was sensitive to body pitch angle shifts at high frequencies. However, this is less important because 38 kHz has been used for the biomass assessment of these fish resources. *S. japonicus* have a swim bladder, which is filled with gas and has a stronger scattering ability than the rest of the fish body. Researchers have shown that the swim bladder accounts for more than 90% of the total scattering of fish with swim bladders (Foote, 1980) and that is why the maximum *TS* of the sample with a body length of 14.81 cm in **Figure 3** appeared at a pitch
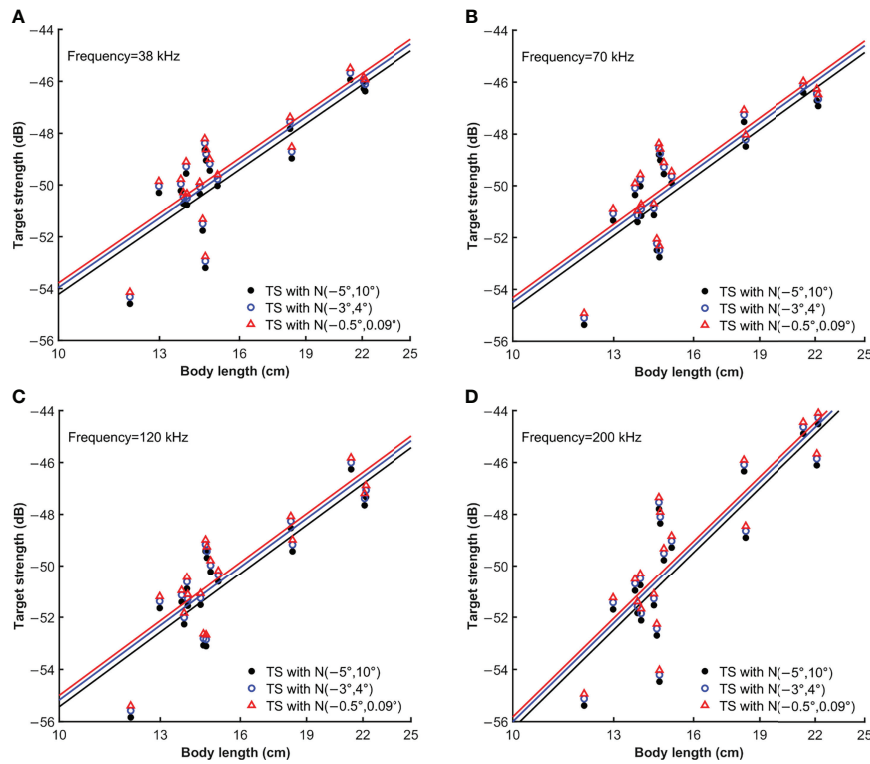
FIGURE 5 | *TS* variation with body length estimated using the measured angle distributions *N*[−3°,4°] and *N*[−0.5°,0.09°], and the universal distribution *N*[−5°,10°] at **(A)** 38 kHz, **(B)** 70 kHz, **(C)** 120 kHz and **(D)** 200 kHz.

angle of about −10°. Because the tilt angle of this sample was 8.4°, the swim bladder reached its normal aspect and intercepted the sound wave the most when the pitch angle was −10°.

Fish have different pitch angles due to differences in body size, swimming speed, and living conditions. In this paper, three pitch angle distributions were used to calculate *TS* of *S. japonicus*. Results show that there were almost no differences between *TS* calculated using the measured *S. japonicus* angle distributions and that estimated by using the universal distribution and this is consistent with the results of Furusawa (1988). Therefore, we

conclude that the difference between the measured and universal angle distributions had little effect on the KRM results for *S. japonicus*. However, due to low samples sizes used to obtain these two measured distributions, *N*[−3°,4°] was observed using four samples and *N*[−0.5°,0.09°] was observed using only one; these conclusions are not generalizable. In addition, these two distributions were quite different, indicating differences in individual swimming patterns. To improve the accuracy of acoustic stock assessment, it is better to estimate *TS* of *S. japonicus* using the measured distribution. It is necessary to carry

TABLE 3 | Equations of the linear regressions plotted in **Figure 5**.

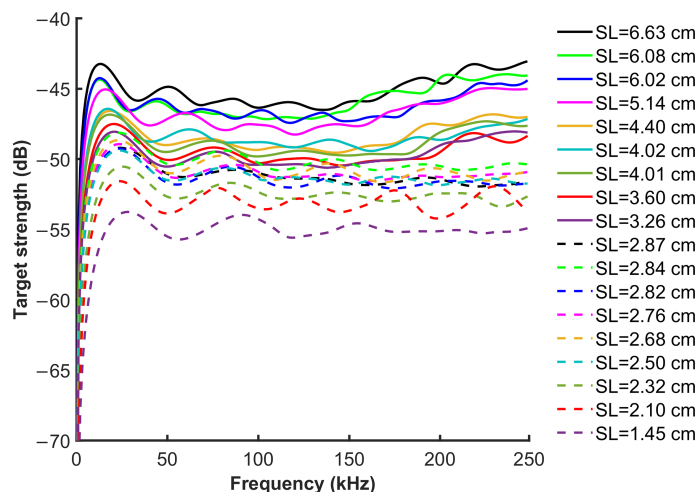| Pitch angle distribution	Frequency (kHz)	$TS = a\log_{10} BL + b$			b_{20}
		a	*b*	r^2	
N[-5°,10°]	38	23.63	-77.85	0.71	-73.53
	70	24.88	-79.65	0.73	-73.82
	120	25.15	-80.59	0.75	-74.44
	200	33.28	-89.56	0.73	-73.72
N[-3°,4°]	38	23.63	-77.6	0.71	-73.27
	70	24.89	-79.39	0.73	-73.56
	120	25.17	-80.35	0.75	-74.18
	200	33.24	-89.25	0.73	-73.46
N[-0.5°,0.09°]	38	23.64	-77.43	0.71	-73.08
	70	24.91	-79.23	0.73	-73.38
	120	25.18	-80.18	0.75	-74
	200	33.24	-89.07	0.73	-73.27

FIGURE 6 | The broadband *TS* spectrum of the 18 *S. japonicus*, was estimated using the pitch angle distribution N[−3°,4°], in the frequency range of 0–250 kHz. The low frequency resonance range is shown, the wide peak is the swim bladder resonance. The solid line refers to the individuals with *SL>3 cm*; the broken line refers to individuals with *SL<3 cm*.

out comprehensive studies on the swimming posture of *S. japonicus* and to use more samples to measure the angle distribution.

There are few studies on TS of *S. japonicus*: Miyanohana et al. (1990) used four frequencies to measure *TS* of *S. japonicus* but they did not show the explicit values. Mukai et al. (1993) measured the b_{20} of individuals with a total length of 23.0–26.8 cm using the *ex situ* method, which was −64.1 dB at 25 kHz and −65.5 dB at 100 kHz. Gutiérrez and Maclennan (1998) reported the b_{20} of *S. japonicus* with a total length of 26–30 cm using the *in situ* method, which was −70.95 dB at 38 kHz and −70.8 dB at 120 kHz. The *TS* calculated using their b_{20} and our total length data were 2–8 dB higher than our KRM model results. Lee and Shin (2005) used the *ex situ* method to obtain the b_{20} for individuals with a total length of 26.2–38.3 cm which was −66.9 dB at 120 kHz and −71.1 dB at 200 kHz. *TS* calculated using their b_{20} were 6–12 dB higher than ours at 120 kHz and 1–7 dB higher at 200 kHz. Svellingen and Charouki (2008, cited in Palermino et al., 2021) used the *in situ* method to measure the b_{20} of *S. japonicus* with an average length of 21.8 cm which was −77.6 dB at 38 kHz and −79.8 dB at 120 kHz. Our *TS* were 0–6 dB higher than results calculated using their b_{20}. Kurnia et al. (2011) reported that the *TS* of a *S. japonicus* with *BL*=21.4 cm was −40.02 dB at 50 kHz when the incidence wave was perpendicular to the dorsal aspect. While the sample with *BL*=21.33 cm in this paper had a simulated *TS* of −36.28 dB under the same frequency and pitch angle. These difference of these results indicate that there may be errors in the KRM estimation. However, the length of *S. japonicus* in most studies was larger than ours, which may be another reason that caused these differences in *TS*.

Density contrast value (*g*) and sound speed contrast value (*h*) of a fish's body and swim bladder are not only important parameters in the KRM model but also in most *TS* models. Changes in *g* and *h* will affect the *TS* estimation (Chu and Wiebe, 2005; Kang et al., 2006; Matsukura et al., 2009). The results of Yasuma et al. (2009) showed that using *g* and *h* values in the primary research may lead to an error of about 10 dB when using the deformed cylinder model to

calculate TS of fish without a swim bladder. For zooplankton *TS* estimation, small changes in *g* and *h* in the distorted wave born approximation model can result in errors of up to 20 dB (Chu et al., 2000). Therefore, the use of measured *g* and *h* is better for the accurate estimation of the *TS* of *S. japonicus*. In addition, the results of KRM model are affected by the sound speed and density of seawater. Eulachon (*Thaleichthys pacificus*) has a *TS* of 3–4 dB higher in freshwater than in seawater (Gauthier and Horne, 2004). For fish with a swim bladder, their volume has a greater effect on *TS* than *g* and *h* values (Mukai and Iida, 1996; Gorska and Ona, 2003). Studies showed that some mackerel species have a diel vertical migration behavior (Bertrand et al., 2004; Li et al., 2014; Tsuda et al., 2014; Paramo et al., 2015). They usually aggregate in deeper water during the daytime and move to the surface at night. These differences have strong implications for the estimation of biomass. Therefore, *TS* in different depths should be attended. According to Boyle's law, there is a negative correlation between swim bladder volume and water depth. With increasing depth, pressure increases on the swim bladder causing a decrease in volume and the effective backscattering cross-section, which leads to a decrease in *TS*. Morphological characteristics in this study were obtained by taking X-ray images of fish out of the water. However, *TS* in different depths still needs further study and experimental data on *TS* at different depths are needed to validate the theoretical model.

In recent years, using broadband techniques to identify and classify species in echograms has become a hot topic in fishery acoustics (Stanton et al., 2010; Yan et al., 2020; Hasegawa et al., 2021; Xue et al., 2021). At the same time, a growing number of research vessels are equipped with broadband fish finders. The broadband scattering spectrum of *S. japonicus* produced by us can provide a reference for identifying *S. japonicus* in a mixed population echogram. The two observed trends in *TS* variation of individuals with different swim bladder lengths above 150 kHz

may be related to the ratio of swim bladder lengths to acoustic wavelengths. It is necessary to select the appropriate frequency for the body length of the fish to improve accuracy when using the dB-difference method for stock assessment.

DATA AVAILABILITY STATEMENT

The raw data supporting the conclusions of this article will be made available by the authors, without undue reservation.

ETHICS STATEMENT

The animal study was reviewed and approved by the Institutional Animal Care and Use Committee of Shanghai Ocean University.

AUTHOR CONTRIBUTIONS

FUNDING

ACKNOWLEDGMENTS

REFERENCES

Bairstow, F., Gastauer, S., Finley, L., Edwards, T., Brown, C. T. A., Kawaguchi, S., et al. (2021). Improving the Accuracy of Krill Target Strength Using a Shape Catalogue. *Front. Mar. Sci.* 8. doi: 10.3389/fmars.2021.658384

Bertrand, A., Barbieri, M. A., Cordova, J., Hernandez, C., Gomez, F., and Leiva, F. (2004). Diel Vertical Behaviour, Predator Prey Relationships, and Occupation of Space by Jack Mackerel (*Trachurus Murphyi*) Off Chile. *ICES J. Mar. Sci.* 61, 1105–1112. doi: 10.1016/j.icesjms.2004.06.010

Chiba, S., Sugisaki, H., Nonaka, M., and Saino, T. (2009). Geographical Shift of Zooplankton Communities and Decadal Dynamics of the Kuroshio-Oyashio Currents in the Western North Pacific. *Global Change Biol.* 15, 1846–1858. doi: 10.1111/j.1365-2486.2009.01890.x

Chu, D., and Wiebe, P. (2005). Measurements of Sound-Speed and Density Contrasts of Zooplankton in Antarctic Waters. *ICES J. Mar. Sci.* 62, 818–831. doi: 10.1016/j.icesjms.2004.12.020

Chu, D., Wiebe, P., and Copley, N. (2000). Influence of Material Properties of Zooplankton From Acoustic and Resistivity Measurement. *ICES J. Mar. Sci.* 57, 1128–1142. doi: 10.1006/jmsc.2000.0800

Clay, C. S., and Horne, J. K. (1994). Acoustic Models of Fish: The Atlantic Cod (*Gadus Morhua*). *J. Acoust. Soc Am.* 96, 1661–1668. doi: 10.1121/1.410245

Escobar-Flores, P. C., O'Driscoll, R. L., Montgomery, J. C., Ladroit, Y., and Jendersie, S. (2020). Estimates of Density of Mesopelagic Fish in the Southern Ocean Derived From Bulk Acoustic Data Collected by Ships of Opportunity. *Polar Biol.* 43, 43–61. doi: 10.1007/s00300-019-02611-3

FAO (2020). *The State of World Fisheries and Aquaculture 2020. Sustainability in Action* (Rome: Food and Agriculture Organization).

Foote, K. G. (1980). Importance of the Swimbladder in Acoustic Scattering Fish: A Comparison of Gadoid and Mackerel Target Strengths. *J. Acoust. Soc Am.* 67, 2084–2089. doi: 10.1121/1.384452

Foote, K. G. (1982). Optimizing Copper Spheres for Precision Calibration of Hydroacoustic Equipment. *J. Plankton Res.* 71, 742–747. doi: 10.1121/1.387497

Furusawa, M. (1988). Prolate Spheroidal Models for Predicting General Trends of Fish Target Strength. *J. Acoust. Soc Jp.* 9, 13–24. doi: 10.1250/ast.9.13

Gastauer, S., Scoulding, B., Fässler, S. M., Benden, D. P., and Parsons, M. (2016). Target Strength Estimates of Red Emperor (*Lutjanus Sebae*) With Bayesian Parameter Calibration. *Aquat. Living Resour.* 29, 301. doi: 10.1051/alr/2016024

Gauthier, S., and Horne, J. K. (2004). Acoustic Characteristics of Forage Fish Species in the Gulf of Alaska and Bering Sea Based on Kirchhoff-Approximation Models. *Can. J. Fish. Aquat. Sci.* 61, 1839–1850. doi: 10.1139/f04-117

Gibb, A. C., Dickson, K. A., and Lauder, G. V. (1999). Tail Kinematics of the Chub Mackerel *Scomber Japonicus*: Testing the Homocercal Tail Model of Fish Propulsion. *J. Exp. Biol.* 202, 2433–2447. doi: 10.1242/jeb.202.18.2433

Gorska, N., and Ona, E. (2003). Modelling the Effect of Swimbladder Compression on the Acoustic Backscattering From Herring at Normal or Near-Normal Dorsal Incidences. *ICES J. Mar. Sci.* 60, 1381–1391. doi: 10.1016/S1054-3139(03)00142-5

Gutiérrez, M., and Maclennan, D. (1998). Preliminary Results of *In Situ* Target Strength Measurements of the Main Pelagic Species. BIC Humboldt 9803-05 Cruise From Tumbes to Tacna. *Inf. Inst. Mar Perú.* 135, 16–19.

Hasegawa, K., Yan, N., and Mukai, T. (2021). *In Situ* Broadband Acoustic Measurements of Age-0 Walleye Pollock and Pointhead Flounder in Funka Bay, Hokkaido, Japan. *J. Mar. Sci. Tech.* 29, 2. doi: 10.51400/2709-6998.1076

Hazen, L. E., and Horne, J. K. (2003). A Method for Evaluating the Effects of Biological Factors on Fish Target Strength. *ICES J. Mar. Sci.* 60, 555–562. doi: 10.1016/S1054-3139(03)00053-5

Horne, J. K. (2003). The Influence of Ontogeny, Physiology, and Behaviour on the Target Strength of Walleye Pollock (*Theragra Chalcogramma*). *ICES J. Mar. Sci.* 60, 1063–1074. doi: 10.1016/S1054-3139(03)00114-0

Hwang, K., Yoon, E. A., Lee, K., Lee, H., and Hwang, D. J. (2015). Multifrequency Acoustic Scattering Characteristics of Jack Mackerel by KRM Model. *J. Korean Soc Fish. Ocean Technol.* 51, 424–431. doi: 10.3796/KSFT.2015.51.3.424

Jech, J. M., and Horne, J. K. (2002). Three-Dimensional Visualization of Fish Morphometry and Acoustic Backscatter. *Acoust. Res. Lett. Online.* 3, 35–40. doi: 10.1121/1.1430676

Kang, D., Iida, K., Mukai, T., and Kim, J. (2006). Density and Sound Speed Contrasts of the Japanese Common Squid *Todarodes Pacificus* and Their Influence on Acoustic Target Strength. *Fisheries Sci.* 72, 728–736. doi: 10.1111/j.1444-2906.2006.01211.x

Kang, D., Sadayasu, K., Mukai, T., Iida, K., Hwang, D., Sawada, K., et al. (2004). Target Strength Estimation of Black Porgy *Acanthopagrus Schlegeli* Using Acoustic Measurements and a Scattering Model. *Fisheries Sci.* 70, 819–828. doi: 10.1111/j.1444-2906.2004.00875.x

Khodabandeloo, B., Agersted, M. D., Klevjer, T., Macaulay, G. J., and Melle, W. (2021). Estimating Target Strength and Physical Characteristics of Gas-Bearing Mesopelagic Fish From Wideband *In Situ* Echoes Using a Viscous-Elastic Scattering Model. *J. Acoust. Soc Am.* 149, 673–691. doi: 10.1121/10.0003341

Kurnia, M., Iida, K., and Mukai, T. (2011). Measurement and Modeling of Three Dimensional Target Strength of Fish for Horizontal Scanning Sonar. *J. Mar. Sci. Tech.* 19, 287–293. doi: 10.51400/2709-6998.2194

Kusdinar, A., Hwang, B. K., and Shin, H. O. (2014). Determining the Target Strength Bambood Wrasse (*Pseudolabrus Japonicus*) Using Kirchhoff-Ray Mode. *J. Korean Soc Fish. Ocean Technol.* 50, 427–434. doi: 10.3796/KSFT.2014.50.4.427

Lee, D. J., and Shin, I. H. (2005). Construction of a Data Bank for Acoustic Target Strength With Fish Species, Length and Acoustic Frequency for Measuring Fish Size Distribution. *J. Korean Fish. Soc* 38, 265–275. doi: 10.5657/kfas.2005.38.4.265

Li, Y., Chen, X., Chen, C., Ge, J., Ji, R., Tian, R., et al. (2014). Dispersal and Survival of Chub Mackerel (*Scomber Japonicus*) Larvae in the East China Sea. *Ecol. Model.* 283, 70–84. doi: 10.1016/j.ecolmodel.2014.03.016

Love, R. H. (1978). Resonant Acoustic Scattering by Swimbladder-Bearing Fish. *J. Acoust. Soc Am.* 64, 571–580. doi: 10.1121/1.382009

Lu, H. J., Kang, M., Huang, H. H., Lai, C. C., and Wu, L. J. (2011). Ex Situ and *In Situ* Measurements of Juvenile Yellowfin Tuna *Thunnus Albacares* Target Strength. *Fisheries Sci.* 77, 903–913. doi: 10.1007/s12562-011-0401-4

Matsukura, R., Yasuma, H., Murase, H., Yonezaki, S., Funamoto, T., Honda, S., et al. (2009). Measurements of Density Contrast and Sound-Speed Contrast for Target Strength Estimation of Neocalanus Copepods (*Neocalanus Cristatus* and *Neocalanus Plumchrus*) in the North Pacific Ocean. *Fisheries Sci.* 75, 1377–1387. doi: 10.1007/s12562-009-0172-3

Medwin, H., and Clay, C. S. (1998). *Fundamentals of Acoustical Oceanography* (San Diego: Academic Press).

Miyamoto, H., Vijai, D., Tadokoro, K., Watanabe, T., Fuji, T., and Suyama, S. (2020). Geographic Variation in Feeding of Pacific Saury *Cololabis Saira* in June and July in the North Pacific Ocean. *Fish. Oceanogr.* 29, 558–571. doi: 10.1111/fog.12495

Miyanohana, Y., Ishii, K., and Furusawa, M. (1990). Measurements and Analyses of Dorsal-Aspect Target Strength of Six Species of Fish at Four Frequencies. *Rapp. P.-v. Réun. Cons. Int. Explor. Mer.* 189, 317–324.

Mukai, T., and Iida, K. (1996). Depth Dependence of Target Strength of Live Kokanee Salmon in Accordance With Boyle's Law. *ICES J. Mar. Sci.* 53, 245–248. doi: 10.1006/jmsc.1996.0029

Mukai, T., Sano, N., Iida, K., and Sasaki, S. (1993). Studies on Dorsal Aspect Target Strength of Ten Species of Fish Collected in the East China Sea. *Nippon Suisan Gakk.* 59, 1515–1525. doi: 10.2331/suisan.59.1515

Muñoz, L., Aspillaga, E., Palmer, M., Saraiva, J., and Arechavala-Lopez, P. (2020). Acoustic Telemetry: A Tool to Monitor Fish Swimming Behavior in Sea-Cage Aquaculture. *Front. Mar. Sci.* 7. doi: 10.3389/fmars.2020.00645

Nauen, J. C., and Lauder, G. V. (2002). Hydrodynamics of Caudal Fin Locomotion by Chub Mackerel, *Scomber Japonicus* (Scombridae). *J. Exp. Biol.* 205, 1709–1724. doi: 10.1242/jeb.205.12.1709

Ona, E. (2003). An Expanded Target-Strength Relationship for Herring. *ICES J. Mar. Sci.* 60, 493–499. doi: 10.1016/S1054-3139(03)00031-6

Palermino, A., De Felice, A., Canduci, G., Biagiotti, I., Costantini, I., Malavolti, S., et al. (2021). First Target Strength Measurement of *Trachurus Mediterraneus* and *Scomber Colias* in the Mediterranean Sea. *Fish. Res.* 240, 105973. doi: 10.1016/j.fishres.2021.105973

Paramo, J., Lang, C., and Lillo, S. (2015). "Modelled Day-Night Biases in Spatial Structure of Jack Mackerel (*Trachurus Murphyi*) in Chile," in *2015 IEEE/OES Acoustics in Underwater Geosciences Symposium (RIO Acoustics)*. 1–4 (IEEE). doi: 10.1109/RIOAcoustics.2015.7473625

Proud, R., Handegard, N. O., Kloser, R. J., Cox, M. J., and Brierley, A. S. (2019). From Siphonophores to Deep Scattering Layers: Uncertainty Ranges for the Estimation of Global Mesopelagic Fish Biomass. *ICES J. Mar. Sci.* 76, 718–733. doi: 10.1093/icesjms/fsy037

Scoulding, B., Chu, D., Ona, E., and Fernandes, P. G. (2015). Target Strengths of Two Abundant Mesopelagic Fish Species. *J. Acoust. Soc. Am.* 137, 989–1000. doi: 10.1121/1.4906177

Simmonds, J., and MacLennan, D. N. (2005). *Fisheries Acoustics: Theory and Practice, 2nd Ed* (Hoboken: Blackwell Publishing).

Sobradillo, B., Boyra, G., Martinez, U., Peña, M., and Irigoien, X. (2019). Target Strength and Swimbladder Morphology of Mueller's Pearlside (*Maurolicus Muelleri*). *Sci. Rep.* 9, 1–14. doi: 10.1038/s41598-019-53819-6

Sobradillo, B., Boyra, G., Pérez-Arjona, I., Martinez, U., and Espinosa, V. (2021). *Ex Situ* and *in Situ* Target Strength Measurements of European Anchovy in the Bay of Biscay. *ICES J. Mar. Sci.* 78, 782–796. doi: 10.1093/icesjms/fsaa242

Stanton, T. K., Chu, D., Jech, J. M., and Irish, J. D. (2010). New Broadband Methods for Resonance Classification and High-Resolution Imagery of Fish With Swimbladders Using a Modified Commercial Broadband Echosounder. *ICES J. Mar. Sci.* 67, 365e78. doi: 10.1093/icesjms/fsp262

Stierhoff, K. L., Zwolinski, J. P., and Demer, D. A. (2019). *Distribution, Biomass, and Demography of Coastal Pelagic Fishes in the California Current Ecosystem During Summer 2019 Based on Acoustic-Trawl Sampling* (Washington: NOAA).

Sun, Y., Tang, Y., Xing, B. B., Li, H. Q., Bi, F. Y., and Ma, Z. (2021). Target Strength of Northern Whitefish *Coregonus Peled* by Using Kirchhoff Ray Mode Methods. *J. Dalian Ocean. Uni.* 36, 310–316. doi: 10.16535/j.cnki.dlhyxb.2020-082

Svellingen, I. K., and Charouki, N. (2008). "Acoustic Target Strength of Chub Mackerel (*Scomber Japonicus*) Measured *In Situ* Using Split Beam Acoustics," in *Science And Management Of Small Pelagics*. Casablanca, Morocco: Food and Agriculture Organization. pp 11–14.

Takahashi, M., Yoneda, M., Kitano, H., Kawabata, A., and Saito, M. (2014). Growth of Juvenile Chub Mackerel *Scomber Japonicus* in the Western North Pacific Ocean: With Application and Validation of Otolith Daily Increment Formation. *Fisheries Sci.* 80, 293–300. doi: 10.1007/s12562-013-0698-2

Tsuda, Y., Yamamoto, S., Yamaguchi, H., Ohnishi, T., Sakamoto, W., and Murata, O. (2014). Vertical Movement of Spawning Cultured Chub Mackerel (*Scomber Japonicus*) in a Net-Cage. *Aquaculture* 422, 136–140. doi: 10.1016/j.aquaculture.2013.12.008

Xue, M. H., Tong, J. F., Tian, S. Q., and Wang, X. F. (2021). Broadband Characteristics of Zooplankton Sound Scattering Layer in the Kuroshio–Oyashio Confluence Region of the Northwest Pacific Ocean in Summer of 2019. *J. Mar. Sci. Eng.* 9, 938. doi: 10.3390/jmse9090938

Yan, N., Mukai, T., Yamamoto, J., and Hasegawa, K. (2020). Acoustic Discrimination Between Juvenile Walleye Pollock and Pointhead Flounder. *Fish. Res.* 224, 105434. doi: 10.1016/j.fishres.2019.105434

Yasuma, H., Nakagawa, R., Yamakawa, T., Miyashita and, K., and Aoki, I. (2009). Acoustic Models of Fish: The Atlantic Cod (*Gadus Morhua*). *Fisheries Sci.* 75, 545–552. doi: 10.1007/s12562-009-0172-3

Yasuma, H., Sawada, K., Ohshima, T., Miyashita, K., and Aoki, I. (2003). Target Strength of Mesopelagic Lanternfishes (Family *Myctophidae*) Based on Swimbladder Morphology. *ICES J. Mar. Sci.* 60, 584–591. doi: 10.1016/S1054-3139(03)00058-4

Yasuma, H., Sawada, K., Takao, Y., Miyashita, K., and Aoki, I. (2010). Swimbladder Condition and Target Strength of Myctophid Fish in the Temperate Zone of the Northwest Pacific. *ICES J. Mar. Sci.* 67, 135–144. doi: 10.1093/icesjms/fsp218

Zhang, Y. Q., Li, Y. F., Zhang, L. L., Wu, Z., Zhu, S. L., Li, J., et al. (2020). Site Fidelity, Habitat Use, and Movement Patterns of the Common Carp During its Breeding Season in the Pearl River as Determined by Acoustic Telemetry. *Water.* 12, 2233. doi: 10.3390/w12082233

Conflict of Interest: The authors declare that the research was conducted in the absence of any commercial or financial relationships that could be construed as a potential conflict of interest.

Publisher's Note: All claims expressed in this article are solely those of the authors and do not necessarily represent those of their affiliated organizations, or those of the publisher, the editors and the reviewers. Any product that may be evaluated in this article, or claim that may be made by its manufacturer, is not guaranteed or endorsed by the publisher.